Published in : Polymer Chemistry (2020), vol. 11, pp. 7207-7220
DOI: 10.1039/d0py01255f
Status : Postprint (Author's version)

REVERSIBLE DEACTIVATION RADICAL (CO)POLYMERIZATION OF DIMETHYL METHYLENE OXAZOLIDINONE TOWARDS RESPONSIVE VICINAL AMINOALCOHOL-CONTAINING COPOLYMERS†

Zhuoqun Wang, Christophe Detrembleur and Antoine Debuigne *

Center for Education and Research on Macromolecules (CERM), CESAM Research Unit, University of Liege, Sart-Tilman B6a, 4000 Liege, Belgium.
E-mail: adebuigne@uliege.be
†Electronic supplementary information (ESI) available: Additional NMR, SEC and DSC analyses. See DOI: 10.1039/d0py01255f

Radical polymerization of *exo*-methylene cyclic monomers is a straightforward strategy for preparing polymers with pendant heterocycles used as protective groups for reactive functions. In spite of their availability and possible chemical transformations, so far, methylene oxazolidinones have been disregarded in the field of macromolecular synthesis. This work reports the radical (co)polymerization of 4,4-dimethyl-5-methyleneoxazolidin-2-one (DMOx) and the transformation of the pendant oxazolidinone groups into vicinal amino-alcohol functions. DMOx was produced through an optimized procedure of carboxylative cyclization of dimethylpropargylamine. In addition to the conventional radical (co) polymerization of DMOx, we considered its reversible deactivation radical copolymerization with VAc by organometallic-mediated radical polymerization (OMRP) and reversible addition fragmentation chain transfer (RAFT). The ability of these methods to produce well-defined copolymers was studied as well as their respective reactivity ratios. Finally, the poly(DMOx-*co*-VAc) was converted into vicinal amino-alcohol functional poly(vinyl alcohol)s presenting peculiar multi-responsive behavior, namely pH-, thermal- and metal-ion sensitivity.

Published in : Polymer Chemistry (2020), vol. 11, pp. 7207-7220
DOI: 10.1039/d0py01255f
Status : Postprint (Author's version)

Introduction

Oxazolidin-2-one derivatives have been used in many fields of applications as chiral auxiliaries,[1–5] protective groups,[6,7] intermediates of active pharmaceutical ingredients,[8,9] precursors of polyurethanes,[10–12] and electrolyte additives in batteries,[13] to name a few. These heterocyclic residues have also been valued in polymer science leading to high performance materials with enhanced thermal and chemical stabilities as well as improved mechanical properties by means of their rigid cyclic structure.[14–18] Poly(oxazolidinone)s containing heterocyclic groups in their backbone are produced via step-growth polymerization of diepoxydes/diisocyanates[14,15,19–22] or diepoxyde/diurethane[23,24] pairs and, more recently, by rearrangement of poly(β-oxo-urethane)s resulting from polyaddition of bis (α-alkylidene cyclic carbonate)s with diamines.[25] Polymers bearing oxazolidin-2-one as the side chain can be obtained by ring opening polymerization of 3-glycidyloxazolidin-2-one[26] or via vinyl-type (co)polymerization of 3-vinyloxazolidin-2-one 1,[27,28] 5-vinyloxazolidin-2-one 2,[29–32] 3-(4-vinylbenzyl)oxazolidin-2-one 3 [33,34] and 3-acryloyloxazolidin-2-one derivatives 4 [28,35,36] (Fig. 1). These functional macromolecules exhibit attractive properties including metal complexation and hydrogen-bonding abilities.[34,37] Finally, coordination polymerization[36] and Lewis-acid-mediated radical homo-[38] and copolymerization[35] of chiral vinyl oxazolidinones **4b–c** give access to stereoregular polymers.

On the other hand, the radical (co)polymerization of exomethylene cyclic monomers is a straightforward strategy for the synthesis of polymers with pendant heterocyclic functional groups including lactones,[39–48] lactams[49–52] and carbonates.[53,54] The reversible deactivation radical polymerization (RDRP) of methylene heterocyclic monomers was also implemented in order to synthesize functional polymers with predictable molar mass and low dispersities. For example, the conjugated α-methylene-γ-butyrolactone (αMγBL) derivatives were (co)polymerized in a controlled manner by atom transfer radical polymerization (ATRP)[55–59] and reversible addition fragmentation chain transfer (RAFT).[60–62] Recently, the controlled (co)polymerizations of vinyl acetate (VAc) with the unconjugated 4,4-dimethyl-5-methylene-1,3-dioxolan-2-one (DMMDO)[53] or γ-methylene-γ-butyrolactone (γMγBL)[63] were achieved by organometallic-mediated radical copolymerization (OMRP). Hydrolysis of the pendant ester and carbonate moieties of P(VAc-co-DMMDO) led to vicinal diol-containing poly (vinyl alcohol) (PVA) with improved solubility whereas hydrolysis of the esters and lactones of P(VAc-co-γMγBL) gave access to unprecedented pH-responsive acid functional PVA.

Considering the potential of methylene heterocycles for the preparation of functional polymers as well as the possible chemical transformations and properties of oxazolidin-2-one, methylene oxazolidinone derivatives appear as very promising building blocks for macromolecular engineering. In spite of their availability, however, the latter have never been considered as

Published in : Polymer Chemistry (2020), vol. 11, pp. 7207-7220
DOI: 10.1039/d0py01255f
Status : Postprint (Author's version)

monomers for the preparation of oxazolidinonebearing polymers. Herein, we explored the radical (co)polymerization of 4,4-dimethyl-5-methyleneoxazolidin-2-one 5 (DMOx) and the transformation of the pendant oxazolidinone groups into responsive vicinal amino-alcohol functions (inset in Fig. 1). After optimizing the synthesis of DMOx from CO_2 and propargyl amine, we considered its conventional radical homopolymerization and copolymerization with VAc. The reversible deactivation radical copolymerization of DMOx and VAc was also performed *via* OMRP[64,65] and RAFT,[66–68] two RDRP techniques of choice for controlling the polymerization of non-conjugated less activated monomers. The resulting well-defined poly(DMOx-*co*-VAc) were then converted into vicinal aminoalcohol functional poly(vinyl alcohol)s whose peculiar pHresponsive behavior was emphasized as well as metal-ion responsiveness.

Fig. 1 *Structures of vinyl oxazolidinones and general strategy.*

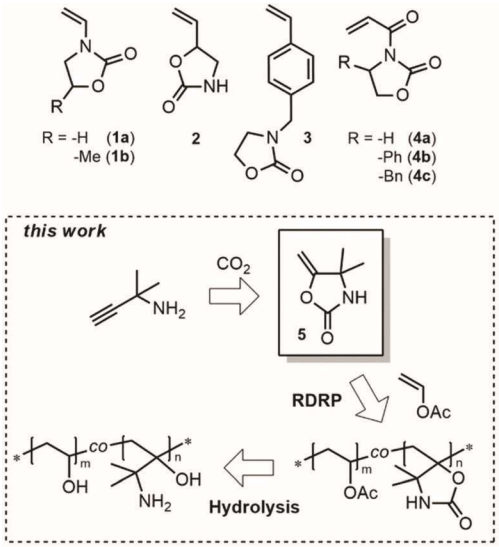

Experimental section

MATERIALS

Cobalt(II) acetylacetonate ($Co(acac)_2$) (97%, Acros), 1,1dimethyl-prop-2-ynylamine (90%, Fluorochem), 2,2,6,6-tetramethylpiperidine 1-oxyl (TEMPO) (98%, Aldrich), 2,2′-azobis(4methoxy-2,4-dimethyl valeronitrile) (V-70, $t^{\frac{1}{2}}$ = 10 h at 30 °C) (>98%, Wako), 2,2′-azobisisobutyronitrile (AIBN) (AIBN, $t^{\frac{1}{2}}$ = 10 h at 65 °C) (98%, Aldrich), *O*-ethyl xanthic acid potassium salt (96%, Aldrich), and methyl bromoacetate (97%, Aldrich) were used as received. Sodium hydroxide (NaOH, ≥97%, Acros), silica gel for column chromatography (60 Å, ROCC S.A.), tetrahydrofuran (THF, ≥99.9%, VWR),

Published in : Polymer Chemistry (2020), vol. 11, pp. 7207-7220
DOI: 10.1039/d0py01255f
Status : Postprint (Author's version)

chloroform (>99%, VWR), methanol (MeOH, ≥99.8%, VWR), n-hexane (>99%, VWR), ethyl acetate (≥99.9%, VWR), and acetonitrile (≥99.99%, Acros) were used as received. Acetone (>99%, VWR), and *N,N*-dimethylformamide (DMF, >99%, VWR) were dried over molecular sieves prior to use. Dichloromethane (CH_2Cl_2) was degassed and dried over 4 Å molecular sieves. Vinyl acetate (VAc) (>99%, Aldrich) was dried under calcium hydride, purified by distillation under reduced pressure and degassed by the freeze–drying cycle under vacuum. The alkyl-cobalt(III) adduct initiator ($PVAc_{<4}$–$Co(acac)_2$, [$Co(acac)_2$–$(CH(OAc)–CH_2)_{<4}R_0$]; R_0 being the primary radical generated by 2,2′-azobis(4-methoxy-2,4-dimethyl valeronitrile) (V-70, Wako) was prepared as described previously[69] and stored as a CH_2Cl_2 solution at −20 °C under argon. Dialyses were carried out with a Spectra/Por dialysis membrane (pretreated RC tubing 1 kDa). A 23 mL Parr bomb reactor (4749 General Purpose Acid Digestion Vessel) was used for the base hydrolysis of the poly (DMOx-*co*-VAc) carried out at 120 °C.

CHARACTERIZATION

Size exclusion chromatography (SEC) of P(DMOX-*co*-VAc) was carried out in DMF containing 0.025 M of LiBr at 55 °C with a Waters chromatograph equipped with three columns (PSS GRAM 1000 Å (×2), 30 Å), a dual λ absorbance detector (Waters 2487) and a refractive index detector (Waters 2414). The system was operated at a flow rate of 1 mL min^{-1}. A polystyrene calibration was used. ^{1}H nuclear magnetic resonance (^{1}H NMR), ^{13}C nuclear magnetic resonance (^{13}C NMR), heteronuclear single quantum coherence (HSQC) and correlation spectroscopy (COSY) spectra were recorded at 298 K with a Bruker Avance III HD spectrometer (B_0 = 9.04 T) (400 MHz) and treated with MestreNova software. Infrared (IR) spectra were recorded on a Thermo Fisher Scientific Nicolet IS5 equipped with an ATR ID5 module using a diamond crystal (650–4000 cm^{-1}). Dynamic light scattering (DLS) was used to obtain the average size of the particles by using a Delsa NanoC instrument. Differential scanning calorimetry (DSC) was performed on a TA Instruments Q1000 DSC, using hermetic aluminum pans, an indium standard for calibration, nitrogen as the purge gas, and a sample weight of about 5 mg. The sample was cooled down to −40 °C at a cooling rate of 40 °C min^{-1}, followed by an isotherm at −40 °C for 2 min and heating up to 200 °C at 10 °C min^{-1} heating rate. This cycle was repeated twice.

Synthesis of 4,4-dimethyl-5-methyleneoxazolidinone (DMOx).

1,1-Dimethyl-prop-2-ynylamine (8.7 g, 104.7 mmol) and $AgNO_3$ (0.089 g, 0.52 mmol) were dissolved in degassed DMSO (11 mL) and heated at 30 °C under 15 bar CO_2 during 4 h. After cooling the reaction mixture to room temperature, the mixture was extracted with $CHCl_3/H_2O$ and purified by column chromatography (hexane/ethyl acetate: 4/1 (v/v)). The crude product was further purified by recrystallization with hexane and ethyl acetate. Accordingly, DMOx was collected as white crystals (10 g) in a 75% yield. ^{1}H NMR (400 MHz, $CDCl_3$): δ 6.92 (s, 1H), 4.63 (d, *J* = 3.4, 1H), 4.21 (d, *J* = 3.3 Hz, 1H), 1.45 (s, 6H). ^{13}C NMR (101 MHz, $CDCl_3$): δ 162.22, 155.75, 84.23, 58.40, 29.37.

Published in : Polymer Chemistry (2020), vol. 11, pp. 7207-7220
DOI: 10.1039/d0py01255f
Status : Postprint (Author's version)

Conventional radical copolymerization of DMOx and VAc.

V-70 (0.093 g, 0.3 mmol) and DMOx (0.25 g, 2.0 mmol) were placed in a 15 mL Schlenk tube under argon. After addition of degassed VAc (0.74 mL, 0.69 g, 8 mmol) and degassed dioxane (0.043 mL, 0.5 mmol) as the internal standard for ^{1}H NMR analysis, the polymerization ($f^{\circ}_{DMOx} = 0.2$) was performed at 40 °C. After 24 h, samples were withdrawn for determining the conversion by ^{1}H NMR in $CDCl_3$ and the molecular parameters (M_n, $Đ$) by SEC in DMF containing 0.025 M of LiBr. The final copolymer was purified via precipitations in diethyl ether (one time) and dialysis in MeOH overnight followed by lyophilization before characterization by ^{1}H NMR, ^{13}C NMR, HSQC and COSY in $CDCl_3$. A similar experiment was carried out with AIBN as the initiator at 65 °C in bulk, keeping constant all other parameters (dioxane (5 mol%), $[comonomers]_0/[initiator]_0 = 100/3$).

Conventional radical homopolymerization of DMOx.

AIBN (0.019 g, 0.12 mmol) and DMOx (0.5 g, 3.93 mmol) were placed in a 15 mL Schlenk tube under argon. After addition of degassed DMF (0.5 mL) and degassed dioxane (0.017 mL, 0.19 mmol) as the internal standard for ^{1}H NMR analysis, the polymerization was performed at 65 °C. After 24 h, samples were withdrawn for determining the conversion by ^{1}H NMR in DMSO-d_6 and the molecular parameters (M_n, $Đ$) by SEC in DMF containing 0.025 M of LiBr. A similar experiment was carried out with V70 as the initiator at 40 °C in DMF, keeping constant all other parameters (dioxane (5 mol%), $[comonomers]_0/[initiator]_0 = 100/3$).

Organometallic-mediated radical copolymerization of DMOx and VAc.

DMOx (0.25 g, 2.0 mmol) was placed in a 15 mL Schlenk tube under argon. A solution of alkyl-cobalt(III) initiator ($PVAc_{<4}$–$Co(acac)_2$) in CH_2Cl_2 (0.16 mL of a 0.122 M stock solution, 0.02 mmol) was added into the same Schlenk tube followed by evaporation of CH_2Cl_2 under reduced pressure at room temperature. Then, degassed VAc (0.74 mL, 0.69 g, 8 mmol) and degassed dioxane (0.04 mL, 0.5 mmol) as the internal standard for ^{1}H NMR analysis were injected under argon. The reaction mixture ($f^{\circ}_{DMOx} = 0.2$ and $f^{\circ}_{VAc} = 0.8$, $[VAc]_0/[DMOx]_0/[PVAc_{<4}–Co(acac)_2]_0 = 400/100/1$) was heated at 40 °C for 36 h. Samples were regularly taken and added to TEMPO in order to quench the polymerization. The monomer conversion was determined by ^{1}H NMR in $CDCl_3$ (1 mg of TEMPO was added per mL of $CDCl_3$). The molecular parameters (M_n, $Đ$) of the polymer were determined by SEC in DMF containing 0.025 M of LiBr (samples were dissolved in DMF containing 10 mg of TEMPO per mL). The polystyrene was used as calibration. After 36 h, the polymerization mixture was quenched by addition of 0.5 mL TEMPO into THF (0.20 g mL^{-1}). The final copolymer was purified by precipitation in diethyl ether (one time) and dialysis in MeOH overnight followed by lyophilization before characterization *via* ^{1}H NMR, ^{13}C NMR, HSQC and COSY in $CDCl_3$.

Similar experiments were carried out with a different monomer initiator ratio ($f^{\circ}_{DMOx} = 0.4$) keeping constant all other parameters (bulk, 40 °C, $[comonomers]_0/[PVAc_{<4}–Co\ (acac)_2]_0 = 500/1$).

Published in : Polymer Chemistry (2020), vol. 11, pp. 7207-7220
DOI: 10.1039/d0py01255f
Status : Postprint (Author's version)

Similar experiments were also carried out at 50 °C keeping constant all other parameters (bulk, $[comonomers]_0/[PVAc_{<4}–Co(acac)_2]_0 = 500/1$).

Determination of reactivity ratios at 40 °C by OMRP.

A series of DMOx/VAc copolymerizations were carried out in bulk at 40 °C with different comonomer ratios $0.1 < (f^{\circ}_{DMOx} = 0.4) < 0.6$ *via* organometallic-mediated radical polymerization ($[comonomers]_0/[PVAc_{<4}–Co(acac)_2]_0 = 500/1$). Copolymerizations were stopped at low conversion in order to avoid significant composition drift. Conversions were determined by ^{1}H NMR in $CDCl_3$. The copolymers were purified by precipitation in diethyl ether (one time) and dialysis in MeOH overnight, and were then lyophilized. The molar fractions of the comonomers in the copolymer (F_{DMOx} and F_{VAc}) were determined by ^{1}H NMR in $CDCl_3$. These data, provided in Table S1,† were then used for the determination of the reactivity ratios via three methods described below.

(i) The Fineman–Ross linearization method[70] which generates a straight line whose slope and intercept with the ordinate (Y-axis) correspond, respectively, to r_1 and r_2 (eqn (1)).

$$f(F-1)/Fr_1(f^2/F) - r_2 \quad (1)$$

where $f = f_1/f_2$ and $F = F_1/F_2$

(ii) The Kelen–Tudos method[71] which involves parameters η and ζ, mathematical functions of the molar ratios in the monomer feed (f) and in the copolymer (F) and of a parameter α calculated on the basis of the lowest and highest values of (f^2/F) The determination of r_1 and r_2 is made possible by the extrapolation and the interception at ξ = 1 and ξ = 0, giving respectively r_1 and $(-r_2/\alpha)$ (eqn (2)).

$$\eta = \left(r_1 + (r_2/\alpha)\right)\zeta - \left(\frac{r_2}{\alpha}\right), \quad (2)$$

where $\eta = (f\,(F-1))/(F(\alpha + (f^2/F))$; $\zeta = (f^2/F)/(\alpha + (f^2/F))$; $\alpha = ((f^2/F)_{max} \times (f^2/F)_{min})^{0.5}$

(iii) The non-linear least squares method[72,73] based on the Mayo–Lewis equation (eqn (3)).

$$F_1 = (r_1 f_1^2 + f_1 f_2)/(r_1 f_1^2 + 2 f_1 f_2 + r_2 f_2^2) \quad (3)$$

Synthesis of methyl (ethoxycarbonothioyl)sulfanyl acetate (xanthate).

In a round-bottom flask, 5 g (3.11 mmol) of the *O*-ethyl xanthic acid potassium salt was dissolved in 20 mL of dry acetone and 4.77 g (2.95 mL, 3.11 mmol) of methyl bromoacetate was then added dropwise. The mixture was stirred at room temperature. After 4 h, the white precipitate of KBr was isolated by filtration and acetone was evaporated off. Finally, a liquid product was purified by column chromatography (hexane/ethyl acetate: 4/1 (v/v)). Yield: 60%. ^{1}H NMR (400 MHz, $CDCl_3$): δ

Published in : Polymer Chemistry (2020), vol. 11, pp. 7207-7220
DOI: 10.1039/d0py01255f
Status : Postprint (Author's version)

4.64 (q, *J* = 7.1 Hz, 2H), 3.92 (s, 2H), 3.75 (s, 3H), 1.41 (t, *J* = 7.2 Hz, 3H). ^{13}C NMR (101 MHz, $CDCl_3$): δ 212.51, 168.40, 70.68, 52.82, 37.67, 13.71.

Reversible addition fragmentation chain transfer copolymerization of DMOx and VAc.

DMOx (0.51 g, 4 mmol), AIBN (0.0044 g, 0.027 mmol) and xanthate (0.026 g, 0.13 mmol) were added into a 15 mL Schlenk tube, and then degassed by three freeze–pump–thaw cycles. The degassed VAc (1.48 mL, 1.38 g, 16 mmol) and degassed dioxane (0.085 mL, 1.00 mmol) as the internal standard for ^{1}H NMR analysis were injected under argon. The reaction mixture ($f^{\circ}_{DMOx} = 0.2$, $[VAc]_0/[DMOx]_0/[xanthate]_0/[AIBN]_0$ = 120/30/1/0.2) was heated at 65 °C for 12 h. Samples were regularly taken to determine conversions by ^{1}H NMR in $CDCl_3$ and molecular parameters (M_n, Đ) of the polymer by SEC in DMF with 0.025 M of LiBr using a polystyrene calibration. After 12 h, the polymerization was stopped by putting the Schlenk tube into liquid nitrogen. The final copolymer was purified by precipitation in diethyl ether (one time) and dialysis in MeOH overnight followed by lyophilization before characterization via ^{1}H NMR, ^{13}C NMR, HSQC and COSY in $CDCl_3$.

Similar experiments were carried out with different monomer initiator ratios ($f^{\circ}_{DMOx} = 0.4$ and $f^{\circ}_{DMOx} = 0.6$) keeping constant all other parameters (65 °C, bulk, $[comonomers]_0/[xanthate]_0/[AIBN]_0$ = 150/1/0.2).

Similar experiments were also carried out with different initial comonomer feed ratios ($[comonomers]_0/[xanthate]_0/[AIBN]_0$ = 500/1/0.2) keeping constant all other parameters

(65 °C, bulk, $f^{\circ}_{DMOx} = 0.2$).

Determination of reactivity ratios at 65 °C by RAFT.

A series of DMOx/VAc copolymerizations were carried out in bulk at 65 °C with different comonomer ratios (0.1 < f°_{DMOx} < 0.6) via reversible addition fragmentation chain transfer polymerization ($[c[omonomers]_0/[xanthate]_0/[AIBN]_0$ = 150/1/0.2). Copolymerizations were stopped at low conversion in order to avoid significant composition drift. Conversions were determined by ^{1}H NMR in $CDCl_3$. The copolymers were purified by precipitation in diethyl ether (one time) and dialysis in MeOH overnight and then lyophilization. The molar fractions of the comonomers in the copolymer (F_{DMOx} and F_{VAc}) were determined by ^{1}H NMR in $CDCl_3$. These data, provided in Table S2,† were then used for the determination of the reactivity ratios *via* three methods aforementioned used in the determination of reactivity ratios at 40 °C by OMRP.

Synthesis of poly(DMOx-*co*-VA).

Poly(DMOx-co-VAc) (0.5 g, 10 000 g mol^{-1}, F_{DMOx} = 0.24) prepared via RAFT ($[VAc]_0/[DMOx]_0/[xanthate]_0/[AIBN]_0$ = 90/60/1/0.2) was dissolved in CH_3CN (5 mL). NaOH (0.5 g, 12.5 mmol) in deionized water (5 mL) was added to the reaction mixture followed by stirring at room

Published in : Polymer Chemistry (2020), vol. 11, pp. 7207-7220
DOI: 10.1039/d0py01255f
Status : Postprint (Author's version)

temperature for 48 h. The pH of the solution was adjusted to pH 7 by addition of HCl (37 wt% in water) followed by dialysis (membrane 1 kDa) against distilled water for 48 h and lyophilization. The poly(DMOx-co-VA) copolymer, recovered as a powder, was characterized by FT-IR and ^{1}H NMR, ^{13}C NMR and HSQC in D_2O.

Synthesis of poly(AMBO-*co*-VA).

Poly(DMOx-*co*-VAc) (0.15 g, 10 000 g mol^{-1}, F_{DMOx} = 0.24) prepared *via* RAFT ($[VAc]_0$/$[DMOx]_0$/$[xanthate]_0$/$[AIBN]_0$ = 90/60/1/0.2) was dissolved in MeOH (1.5 mL). NaOH (0.15 g, 3.75 mmol) in deionized water (1.5 mL) was added to the reaction mixture followed by stirring at 120 °C in a parr bomb reactor for 48 h. Then, HCl (37 wt% in water) was added to adjust the pH of the solution to 7. Subsequently, the solution was dialyzed (membrane 1 kDa) against distilled water for 48 h followed by lyophilization. The poly(AMBO-*co*-VA) copolymer, recovered as a powder, was characterized via ^{1}H NMR, ^{13}C NMR and HSQC in D_2O and FT-IR.

Results and discussion

SYNTHESIS OF THE METHYLENE OXAZOLIDINONE

Over the last few decades, CO_2 has received a lot of interest as abundant C1 feedstock for the preparation of functional molecules including 2-oxazolidinones.[74–76] In particular, the synthesis of alkylidene-oxazolidinones is described by carboxylative cyclization of propargylamines catalyzed by a large variety of organometallic catalysts.[77–81] This strategy was implemented in this work for the synthesis of the methyleneoxazolidinone monomer. In this case, we selected dimethylpropargylamine as the reactant in order to prepare an N–H oxazolidinone monomer able to generate primary amines along the polymer backbone upon hydrolysis, namely 4,4dimethyl-5-methyleneoxazolidin-2-one 5 (DMOx). Note that the methyl groups of the amino precursor should facilitate the ring closure reaction.[82,83] Inspired by the seminal work of Yamada and others,[77,84–86] we carried out the carboxylation of dimethylpropargylamine in DMSO in the presence of a silver catalyst, i.e. 5 mol% of $AgNO_3$ and AgOAc (Table 1, entries 1–3). Compared to these previous reports, however, the reaction was performed under CO_2 pressurized in the absence of a base like DBU (1,8-diazabicycloundec-7-ene) that is suspected to promote the rearrangement of N–H alkylidene-oxazolidinones into tetramic acid derivatives.[87] Under these conditions, near-complete conversion (>98%) of the 1,1-dimethylpropargylamine and selective production of DMOx were observed by ^{1}H NMR, regardless of the nature of the silver catalyst ($AgNO_3$ or AgOAc) and the CO_2 pressure (5 or 15 bar) (Table 1, entries 1–3). Moreover, a blank reaction carried out under 15 bar of CO_2 without a silver compound (Table 1, entry 4) only led to 42% and 92% of amine conversions after 0.5 h and 4 h,

Published in : Polymer Chemistry (2020), vol. 11, pp. 7207-7220
DOI: 10.1039/d0py01255f
Status : Postprint (Author's version)

respectively, which emphasized the key role of the catalyst. Ultimately, DMOx was isolated in 75% yield after 4 h of $AgNO_3$-catalyzed carboxylation of dimethylpropargylamine under 15 bar CO_2 and purification via recrystallization. ^1H and ^{13}C NMR analyses confirmed the structure of DMOx (Fig. S1†).

Table 1. *Synthesis of DMOx via carboxylative cyclization of 1,1-dimethylpropargylamine*

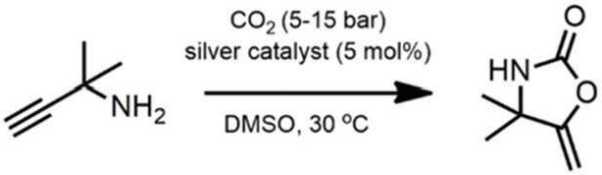

			Conversion[a] (%)		
Entry	Catalyst (5 mol%)	CO_2 (bar)	0.5 h	1h	4h
1	AgOAc	15	98	100	100
2	AgNO3	15	98	97	97
3	AgNO3	5	100	100	100
4	—	15	42	62	92

Conditions: In DMSO at 30 °C. [a]Determined by ^1H NMR.

CONVENTIONAL RADICAL (CO)POLYMERIZATION OF DMOX

Initially, the radical homopolymerization of DMOx was tested at 40 °C or 65 °C in the presence of 2,2′-azobis(4-methoxy-2,4dimethyl valeronitrile) (V70) or azobis-(isobutyronitrile) (AIBN), respectively (scheme in Table 2). Because these temperatures are inferior to the melting point of the monomer (mp = 68.69 °C), we performed the polymerization in solution in DMF (1 g DMOx per mL of DMF). However, no polymerization occurred under these conditions after 48 h (Table 2, entries 1 and 2). The low propensity of DMOx for homopolymerization is certainly due to the steric hindrance of the propagating radical. Therefore, we considered the conventional radical copolymerization of DMOx with a common non-conjugated monomer, *i.e.* vinyl acetate (VAc), at the same temperatures (40 °C or 65 °C) using both classical azo-initiators (V70 or AIBN) (Table 2, entries 3 and 4). Due to the good solubility of DMOx in VAc, these copolymerizations could be performed in bulk. After 24 h of copolymerization conducted at 40 °C in the presence of V70 with an initial molar fraction of DMOx (f°_{DMOx}) of 0.2, the conversion of DMOx and VAc reached 15% and 67%, respectively (Table 2, entry 3). A poly(DMOx-co-VAc) copolymer with low molar mass (*M*n SEC = 5700 g mol−1) and high dispersity (*Đ* = 1.64) was formed accordingly. The ^1H NMR (Fig. S2†) as well as the COSY and HSQC spectra (Fig. S3†) confirmed the presence of both comonomer units in the backbone. The relative intensity of the 1H signals corresponding to the methyl protons e of DMOx at 1.3 ppm and of the methyne hydrogen b of VAc at 5 ppm indicated a molar fraction of DMOx in the copolymer (F_{DMOx}) equal to 0.08. Next, V70 was replaced by AIBN and the temperature was increased to 65 °C (Table 2, entry 4). Following these changes, the copolymerization was faster and the conversion of DMOx reached 66% after 24 h.

Published in : Polymer Chemistry (2020), vol. 11, pp. 7207-7220
DOI: 10.1039/d0py01255f
Status : Postprint (Author's version)

Moreover, the poly(DMOx-*co*-VAc) molar mass (27 700 g mol^{-1}) and its content in DMOx (F_{DMOx} = 0.14) increased.

OMRP COPOLYMERIZATION OF DMOX

In the perspective of the precision design of the DMOx-containing copolymers, we investigated the reversible deactivation radical copolymerization of DMOx and VAc. For this purpose, we first considered the organometallic-mediated radical polymerization (OMRP), a method known for its efficiency to control the radical polymerization of the less activated monomers (LAMs), in particular VAc.[69,88] For this purpose, we selected an alkyl-Co(acac)$_2$ derivative, i.e. PVAc$_{<4}$–Co(acac)$_2$, as the OMRP initiator for the DMOx/VAc copolymerization (Fig. 2). Table 3 gathers data for such copolymerizations carried out from different comonomer feed ratios and various temperatures.

The first copolymerization trials were carried out in bulk at 40 °C (Table 3, entries 1 and 2), which corresponds to the optimized temperature for the Co(acac)$_2$-mediated homopolymerization of VAc.[69] Two initial monomer feed ratios were used, *i.e.* f°_{DMOx} of 0.2 and 0.4 (Table 3, entries 1 and 2). In these cases, the conversion of both comonomers increased with the time confirming the formation of the poly(DMOx-co-VAc) copolymers. Overall, these polymerizations were significantly slower compared to the OMRP of VAc[69] and the DMOx/VAc copolymerization rate significantly decreased when increasing the DMOx content in the feed. After about 35 h, conversions of 36% and 21% were observed for f°_{DMOx} equal to 0.2 and 0.4, respectively. In both cases, the M_n of the copolymer regularly increased with the conversion as expected for a controlled polymerization process. Moreover, the dispersity of the poly(DMOx-*co*-VAc)s was low at the early stage of the reaction ($Đ$ < 1.2) and increased along the reaction ($Đ$ ~ 1.4). Indeed, the SEC chromatograms revealed the appearance of a tailing on the low molar mass side of the peaks that is due to irreversible terminations occurring during the polymerization (Fig. 3). Note that the SEC traces of the final copolymers exhibit a small shoulder at low elution time that likely corresponds to few percent of coupling of the chains occurring during the isolation of the copolymers, as observed in previous OMRP studies.[89] The molar masses of the polymers were also measured by ^{1}H NMR by taking into account the relative intensity of the repeating units and the terminal methoxy function (Table 3 and Fig. S4a†). Some deviation appeared between the $M_{n\ NMR}$ and $M_{n\ th}$, likely due to the occurrence of termination reactions, but overall these values remained in the same range (Table 3). Finally, the poly(DMOx-co-VAc)s were analyzed by ^{1}H NMR, COSY and HSQC, as illustrated in Fig. S4,† in order to confirm their structure and evaluate their composition. As expected, when the initial molar fraction of DMOx (f°_{DMOx}) increased from 0.2 to 0.4, the content of DMOx units in the copolymer (F_{DMOx}) increased from approximately 0.10 to 0.20.

In order to improve the rate of the DMOx/VAc copolymerization, we repeated the same experiments at a higher temperature, *i.e.* 50 °C. For both initial comonomer feed ratios, the dependence of the

Published in : Polymer Chemistry (2020), vol. 11, pp. 7207-7220
DOI: 10.1039/d0py01255f
Status : Postprint (Author's version)

ln$[M]_0/[M]$ functions with the time at 40 °C and 50 °C highlighted a drastic increase of the polymerization rate with the temperature (Fig. 4A and S5A†). Indeed, about 30% conversion was reached after only 4 h at 50 °C compared to 16 h at 40 °C (Table 3, entries 1 and 3). Regardless of the temperature, however, the copolymerization significantly slowed down beyond 30% conversion (Fig. 4A and S5A†). This phenomenon certainly results from irreversible termination reactions, assessed by the tailing on the SEC chromatograms (Fig. 3 and S6†), leading to the accumulation of the cobalt(II) deactivator in the polymerization medium. Note that the enrichment in DMOx resulting from the preferential incorporation of VAc into the copolymer might also account for the observed decrease of the polymerization rate with the reaction time. Nevertheless, quite similar dependence of M_n and Đ on monomer conversion was observed at 40 °C and 50 °C (Fig. 4B and S5B†), which supports the control character of the copolymerization at both temperatures. Finally, increasing the polymerization temperature by 10 °C did not significantly modify the composition of the copolymers; at 50 °C, F_{DMOx} reached 0.12 and 0.22 for f°_{DMOx} of 0.2 to 0.4, respectively (Table 3, entries 3 and 4).

Reactivity ratios for the DMOx/VAc pair were determined by Fineman–Ross[70] (FR, Fig. 5B), Kelen–Tudos[71] (KT, Fig. 5C) and nonlinear least-squares fitting[72,73] (NL, Fig. 5A) in order to gain insight into the comonomer distribution. For this purpose, a series of copolymerizations with different initial feed compositions (f°_{DMOx} ranging from 0.1 to 0.6) were carried out by OMRP in bulk at 40 °C (Table S1†). For each experiment, TEMPO was added timely to ensure low conversion and prevent significant composition drift and the copolymer compositions were measured by ^{1}H NMR. The reactivity ratios obtained by the three methods were consistent. The average r_{VAc} value is equal to 1.49 emphasizing the ability of the VActerminated radical chains to react with both comonomers. In contrast, we measured a r_{DMOx} equal to 0 confirming the inability of DMOx for self-propagation. This conclusion is consistent with the failure to produce homopoly(DMOx) by conventional radical polymerization at the same temperature.

Considering the low propensity of DMOx for self-propagation, performing its controlled radical copolymerization with VAc at higher temperature is appealing. Nevertheless, the $Co(acac)_2$–carbon bonds involved in the OMRP equilibrium are too weak above 50 °C to ensure proper control of the polymerization of VAc,[90] which led us to consider another RDRP method that operates at higher temperature, namely reversible addition–fragmentation chain transfer polymerization (RAFT).

Published in : Polymer Chemistry (2020), vol. 11, pp. 7207-7220
DOI: 10.1039/d0py01255f
Status : Postprint (Author's version)

Fig. 2. *Organometallic-mediated radical (co)polymerization of DMOx and VAc.*

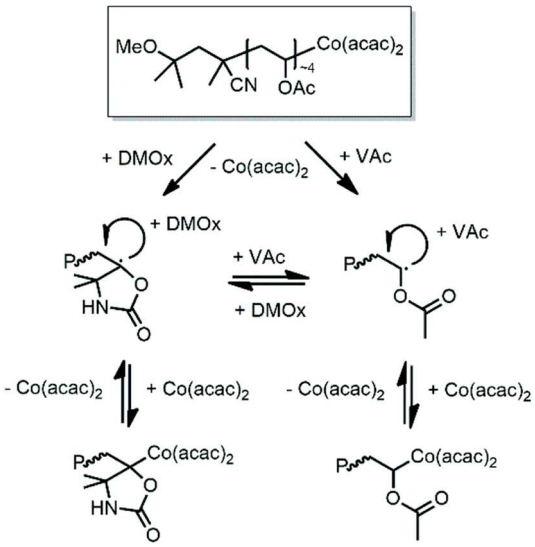

Table 2. *Conventional radical homo- and copolymerization of DMOx*

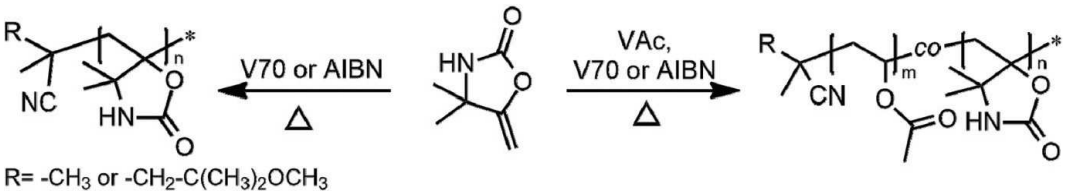

Entry	Initiator	Temp (°C)	f°_{DMOx}	f°_{VAc}	Conv. (%)[c] DMOx	Conv. (%)[c] VAc	$M_{n\,SEC}$[d] (g mol^{-1})	$Đ$[d]	F_{DMOx}[e]
1	V70[a]	40	1	0	—	—			
2	AIBN[a]	65	1	0	—	—	—	—	—
3	V70[b]	40	0.20	0.80	15	67	5700	1.64	0.08
4	AIBN[b]	65	0.20	0.80	66	92	27 700	1.73	0.14

Conditions: [initiator]/[comonomers] = 3/100. [a] Carried out in DMF solution (1 g DMOx per mL of DMF). [b] Performed in bulk. [c] Determined by 1H NMR in $CDCl_3$. [d] Determined by SEC in DMF/LiBr using a PS calibration. [e] Determined by ^{1}H NMR in $CDCl_3$ after purification.

Published in : Polymer Chemistry (2020), vol. 11, pp. 7207-7220
DOI: 10.1039/d0py01255f
Status : Postprint (Author's version)

Table 3. *Organometallic-mediated radical (co)polymerization of DMOx and VAc*

				Conv[a] (%)							
Entry	*T* (°C)	f°_{DMOx}	Time (h)	DMOx	VAc	Total	$M_{n\,SEC}$ [b] (g mol $^{-1}$)	$Đ$ [b]	F_{DMOx} [c]	$M_{n\,th}$ [d] (g mol $^{-1}$)	$M_{n\,NMR}$ [c] (g mol $^{-1}$)
1	40	0.20	2	3	9	8	4200	1.08			
			4	6	19	16	5900	1.08			
			8	9	24	21	9600	1.10			
			12	11	32	28	11 800	1.13			
			16	14	37	32	14 700	1.13			
			20	16	39	34	16 700	1.24			
			36	17	41	36	17 700	1.42	0.10	16 300	11 400
2	40	0.40	2	3	7	6	4900	1.10			
			4	3	13	9	7700	1.13			
			8	4	20	14	11 600	1.18			
			12	4	25	17	14 400	1.25			
			18	7	28	19	17 400	1.37			
			34	7	30	21	19 200	1.38	0.20	9500	8600
3	50	0.20	1	0	19	15	6600	1.07			
			2	9	28	24	10 400	1.08			
			3	11	31	27	12 500	1.12			
			4	12	36	31	14 700	1.15			
			6	14	43	37	17 100	1.23			
			8	15	44	38	20 800	1.32			
			10	18	44	39	22 500	1.38	0.12	17 000	11 700
4	50	0.40	2	7	17	13	9100	1.13			
			4	8	22	16	12 800	1.20			
			6	9	26	19	15 100	1.29			
			8	9	30	22	16 600	1.38			
			10	10	31	23	16 700	1.40	0.22	10 500	7600

Conditions: 40 °C or 50 °C, [RCo]/[comonomers] = 1/500. [a] Determined by ^{1}H NMR in $CDCl_3$. [b] Determined by SEC in DMF/LiBr using a PS cali¬bration. [c] Determined by ^{1}H NMR in $CDCl_3$ (f°_{DMOx}= 0.2) or DMSO-d_6 (f°_{DMOx} = 0.4) after purification. $M_{n\,NMR}$ is measured considering the CH_3O- chain-end signal f (Fig. S4a†). [d] Theoretical molar mass ($M_{n\,th}$) calculated based on the [monomer]/[RCo] ratio and the conversion.

Published in : Polymer Chemistry (2020), vol. 11, pp. 7207-7220
DOI: 10.1039/d0py01255f
Status : Postprint (Author's version)

Fig. 3 *SEC traces for the OMRP of DMOx and VAc performed at 40 °C with* f°_{DMOx} *equal to (A) 0.2 and (B) 0.4 (Table 3, entries 1 and 2).*

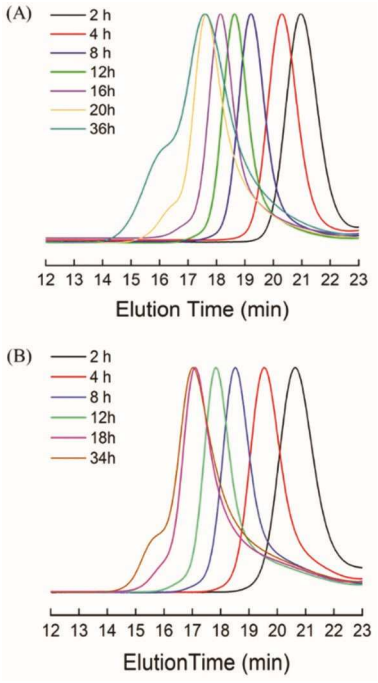

Fig. 4 *(A) Time dependence of ln[M]$_0$/[M] and (B) dependence of M_n (full symbols) and Đ (hollow symbols) on the total monomer conversion for the OMRP of DMOx and VAc (*f°_{DMOx} *= 0:2, [DMOx]/[VAc]/[RCo] = 100/400/1) at 40 °C (■) and 50 °C (▲).*

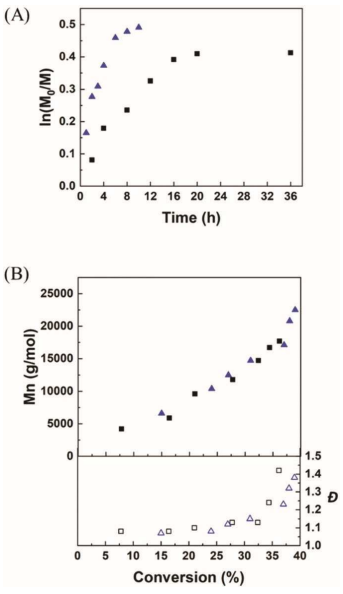

Published in : Polymer Chemistry (2020), vol. 11, pp. 7207-7220
DOI: 10.1039/d0py01255f
Status : Postprint (Author's version)

Fig. 5 *Determination of the reactivity ratios for the bulk copolymerization DMOx and VAc by OMRP at 40 °C (A–C) and by RAFT at 65 °C (E–G) via the non-linear (A and E), Fineman–Ross (B and F) and Kelen–Tudos (C and G) methods. E xperimental data are presented in Tables S1 and S2.†*

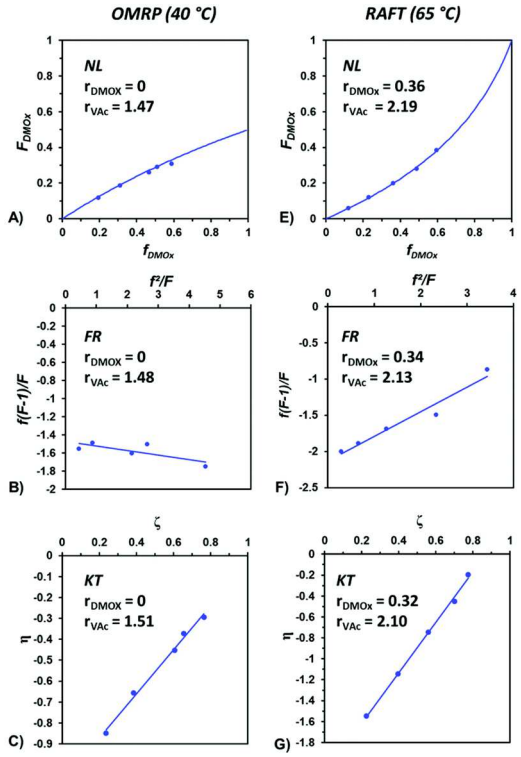

RAFT COPOLYMERIZATION OF DMOX

Nowadays, RAFT is considered as one of the most robust and versatile RDRP methods due to its compatibility with several reaction media and its applicability to a wide range of monomers including LAMs.[67,91–93] In particular, proper control of the polymerization of vinyl esters is described above 60 °C when using *O*-alkyl xanthates as RAFT agents.[68,93–95] In the light of these considerations, we studied the RAFT copolymerization of DMOx and VAc and selected a xanthate known for its ability to control the polymerization of VAc, *i.e.* methyl(ethoxycarbonothioyl)sulfanyl acetate[94] (scheme in Table 4). This xanthate was prepared following a previously reported procedure[94] and characterized by ^{1}H and ^{13}C NMR (Fig. S7†). The RAFT copolymerization of DMOx and VAc was implemented with different feed compositions and comonomer/xanthate ratios (Table 4).

The copolymerizations of DMOx and VAc were carried out in bulk at 65 °C in the presence of the RAFT agent and 0.2 equivalent of AIBN. In order to evaluate the ability of this system to produce well-defined poly(DMOx-co-VAc)s with predictable molar masses, two different monomer/xanthate molar ratios, i.e. 500 and 150, were tested for the same comonomer feed composition $f^{\circ}_{DMOx} = 0.2$

Published in : Polymer Chemistry (2020), vol. 11, pp. 7207-7220
DOI: 10.1039/d0py01255f
Status : Postprint (Author's version)

(Table 4, entries 1 and 2). In both cases, 45% conversion was reached in less than 10 h and the copolymerizations were properly controlled as indicated by the linear increase of the M_n with the monomer conversion, the low dispersity of the copolymers ($Đ\sim$ 1.2–1.3) (Fig. 6A) and the regular shift of the symmetrical SEC peaks with the time (Fig. 6B). For a given conversion, the M_n of poly(DMOx-*co*-VAc) significantly changed with the monomer/xanthate molar ratio.

As expected, higher $M_{n\ SEC}$ were obtained for a $[monomer]_0/[xanthate]_0$ ratio of 500 (Fig. 6A). Moreover, the experimental molar masses of the final copolymers determined by NMR are in agreement with the theoretical values calculated based on the $[monomer]_0/[xanthate]_0$ ratio and the conversion (Table 4). Importantly, the copolymerization preserves its controlled character at least until 66% conversion. The resulting copolymers were analyzed by ^{1}H, COSY and HSQC experiments (Fig. S8†). Besides signals of the comonomer units, characteristic peaks of the RAFT agent like the methyl group h (C$\underline{H}_3$– OCO–) and the methylene group f (–C$\underline{H}_2$–O(CvS)–S–) were detected at 3.6 ppm and 4.7 ppm, respectively. According to the relative intensities of the ^{1}H signals of the comonomer units, the incorporation of DMOx into the copolymer reached about 12 mol%.

A longer polymerization time was also considered for the RAFT copolymerization of DMOx/VAc (f°_{DMOx} = 0:2, $[monomer]_0/[xanthate]$ = 150). After 24 h, the total monomer conversion reached 70% and the resulting poly(DMOx-co-VAc) showed quite similar macromolecular parameters ($M_{n\ SEC}$ = 13 000 g mol^{-1}, $Đ$ = 1.36, F_{DMOx} = 0.12) compared to the copolymer obtained after 12 h (Table 4, entry 2). The difficulty in reaching higher conversions in this case certainly results from a drastic slowdown of the polymerization when the amount of DMOx increases in the medium.

Next, we varied the DMOx/VAc feed composition (f°_{DMOx} = 0.2, 0.4 and0.6) while keeping a $[monomer]_0/[xanthate]_0$ equal to 150 (Table 4, entries 2–4). Regardless of the initial comonomer ratio, the copolymerization proceeded in a controlled manner as illustrated by Fig. S9A and S10.† Similarly to OMRP, increasing the DMOx content in the feed markedly decreased the rate of the RAFT copolymerization (Fig. S9B†). Expectedly, the DMOx molar fraction in the copolymer increased along with the proportion of this comonomer in the feed; up to 41 mol% of DMOx units could be inserted in the copolymer for f°_{DMOx} equal to 0.6.

Finally, the reactivity ratios were also determined for the RAFT copolymerization of DMOx/VAc in bulk at 65 °C. For this purpose, a series of experiments were conducted in the presence of methyl(ethoxycarbonothioyl)sulfanyl acetate and 0.2 equivalent of AIBN using different feed compositions (f°_{DMOx} ranging from 0.1 to 0.6) (Table S2†). After measuring the copolymer compositions by ^{1}H NMR at low monomer conversion, reactivity ratios were determined by FR[70] (Fig. 5F), KT[71] (Fig. 5G) and nonlinear[72,73] least-squares fitting (NL) (Fig. 5E) methods. The average values for r_{VAc} and r_{DMOx} were equal to 2.14 and 0.34, respectively, which confirmed the preferential incorporation of VAc within the poly(DMOx-co-VAc)s copolymers. In contrast to the OMRP carried out

Published in : Polymer Chemistry (2020), vol. 11, pp. 7207-7220
DOI: 10.1039/d0py01255f
Status : Postprint (Author's version)

at 40 °C, however, r_{DMOx} for RAFT at 65 °C is not zero. This minor propensity for self-addition might also account for the ability of the RAFT process to proceed with a high DMOx content.

SYNTHESIS AND STIMULI-RESPONSIVE PROPERTIES OF MODIFIED PVOH

2-Oxazolidinone groups are useful protective groups and intermediates in the synthesis of vicinal amino alcohol derivatives.[6,96] Their conversion into amino alcohols typically requires the use of a hydroxide base in a water/organic cosolvent mixture.[6,96] On the other hand, the base hydrolysis and methanolysis of PVAc are widely used in the production of PVA,[97–99] an industrial polymer used in many fields including biological applications.[100,101] In the light of these considerations, the P(DMOx-*co*-VAc) copolymers were tentatively hydrolyzed in order to prepare unprecedented PVAs containing vicinal amino alcohol moieties along their backbone. The protonability of the amines and the H-bonding capacity of both alcohol and amino groups are expected to impart peculiar pH and thermal responsiveness to these modified PVAs. Because the hydrolysis of *N*-unsubstituted oxazolidinones often necessitates harsh thermal treatment,[96] it should be possible to promote the selective hydrolysis of the esters or the complete transformation of both ester and oxazolidinone functions at low and high temperature, respectively (Fig. 7). In practice, a RAFT synthesized P(DMOx-*co*-VAc) (10 000 g mol^{-1}, $Đ$ = 1.27) containing 24 mol% of DMOx was treated with sodium hydroxide for 48 h at different temperatures, *i.e.* 25 °C and 120 °C (Fig. 7A).

As anticipated, selective hydrolysis of the ester functions of the poly(DMOx-*co*-VAc) occurred upon treatment with NaOH at r.t. for 48 h in a CH_3CN/water mixture leading to a PVA with pendant oxazolidinones moieties, namely P(DMOx-*co*-VA). The conversion of the esters into alcohol functions was confirmed by the appearance of the O–H stretching IR band at 3300 cm^{-1} and the disappearance of the characteristic C–O–C ester band at 1228 cm^{-1} while the oxazolidinone peak around 1730 cm^{-1} was preserved (Fig. 7B). In contrast, the latter IR signal also disappeared when P(DMOx-co-VAc) was reacted with NaOH at 120 °C in a MeOH/water mixture confirming the full hydrolysis of both esters and oxazolidinone rings and the production of the desired P(AMBO-co-VA), namely poly(3-amino-3-methylbut1-en-2-ol-co-vinyl alcohol). Additional proofs of the formation of the partially hydrolyzed P(DMOx-co-VA) and the fully hydrolyzed P(AMBO-*co*-VA) are provided by ^{1}H (Fig. 8), ^{13}C (Fig. S11†) and HSQC (Fig. S12†) NMR analyses. For example, ^{13}C NMR spectra showed the selective disappearance of the ester signal –$\underline{C}O_2CH_3$ at 170 ppm for the room temperature hydrolysis and the concomitant loss of the peaks assigned to the ipso carbons of the ester and oxazolidinone functions at 170 ppm and 157 ppm for the reaction performed at 120 °C (Fig. S11†). The thermal properties of these copolymers were also analyzed by DSC (Fig. S13†). As a result of the incorporation of rigid oxazolidinone groups along the polymer backbone, the T_g markedly increased from about 30 °C for a classical PVAc homopolymer to 116 °C for the P(DMOx-co-VAc) with 24 mol% of DMOx. The glass

Published in : Polymer Chemistry (2020), vol. 11, pp. 7207-7220
DOI: 10.1039/d0py01255f
Status : Postprint (Author's version)

transition temperature of the copolymer further increased upon hydrolysis; T_g of 147 °C and 161 °C were determined for P(DMOx-co-VA) and P(AMBO-*co*-VA), respectively (Fig. S13†).

Finally, exploring the solution behavior of the fully hydrolyzed poly(AMBO-*co*-VA) not only emphasized the pH-responsiveness of the latter via protonation–deprotonation of the amino groups but also highlighted the influence and thermal dependence of H-bonding (Fig. 9). At pH 1, the amine moieties of poly(AMBO-*co*-VA) are mainly in their protonated state which favors the solubility of the copolymer in water; some objects with a low mean diameter (~48 nm) are observed under these conditions by dynamic light scattering (DLS) most probably as a result of some H-bond interactions. As anticipated, basification of this solution to pH 11 via NaOH addition significantly affected the solubility of the poly(AMBO-*co*-VA) due to the deprotonation of its amino groups as assessed by the assembly of objects with a diameter superior to 1 µm. Note that the solution remained clear suggesting the formation of loose and hydrated aggregates rather than densely packed particles. Interestingly, these large size objects were preserved when the poly(AMBO-*co*-VA) solution was reacidified to pH 1 and only fell apart after heating the solution at 80 °C for 2 h. This thermal treatment certainly accounts for the rupture of the H-bonding network which favors the solubilization of the vicinal amino alcohol-containing copolymer chains. A similar behavior was observed for the P(AMBO-*co*-VA) solution for a second pH- and thermal-stimulation cycle.

Considering the known ion chelating ability of polyamines and their applications in sensor ion and heavy metal recovery,[102,103] the metal-ion sensitivity of the amino-containing P(AMBO-co-VA) copolymer was examined (bottom Fig. 9). Typically, an aqueous solution of P(AMBO-*co*-VA) (2.5 mg mL^{-1}) in its deprotonated state at pH 11 was added to $CuCl_2$ (2 mg dissolved in 0.1 mL of water). Under these conditions, the chelation of Cu^{2+} ions by the pendant amino groups promoted the crosslinking of the chains and the deposition of colored Cu-loaded aggregates in few minutes (Fig. 9).

Interestingly, this deposit completely dissolved upon acidification of the medium to pH 1 as a result of the protonation of the amines and dechelation of the Cu^{2+} ions. No aggregate was detected by DLS in the resulting colorless solution which mainly contains P(AMBO-*co*-VA) as free chains. Regarding the absence of objects in this case, we hypothesize that a large portion of the amino groups are involved in the complexation of Cu^{2+} ions rather than in H-bonding before acidification which limits the persistence of objects when the pH of the solution is decreased to 1. It is worth noting that the pH-triggered chelation of Cu^{2+} by P(AMBO-*co*-VA) is reversible which is advantageous in the perspective of metal recovery and ionsensor applications.

Published in : Polymer Chemistry (2020), vol. 11, pp. 7207-7220
DOI: 10.1039/d0py01255f
Status : Postprint (Author's version)

Table 4 *RAFT copolymerization of DMOx and VAc*

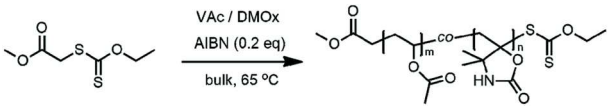

Entry	[Monomers]/[xanthate]	f°_{DMOx}	Time (h)	Conv[a] (%) DMOx	VAc	Total	$M_{n\,SEC}$ [b] (g mol^{-1})	$Đ$ [b]	F_{DMOx} [c]	$M_{n\,th}$ [d] (g mol^{-1})	$M_{n\,NMR}$ [c] (g mol^{-1})
1	500	0.2	2	8	11	10	5500	1.35			
			4	12	23	21	9800	1.28			
			6	16	31	28	13 900	1.25			
			8	19	38	34	17 000	1.24			
			10	26	50	45	21 200	1.23			
			12	27	52	47	22 400	1.21	0.13	21 000	17 300
2	150	0.2	2	13	10	11	3600	1.24			
			4	17	21	20	5400	1.22			
			6	19	34	31	7700	1.19			
			8	22	40	36	9600	1.20			
			10	25	54	48	10 800	1.25			
			12	32	74	66	11 900	1.29	0.12	8900	10 400
3	150	0.4	2	3	4	4	2100	1.13			
			4	6	12	10	2700	1.21			
			6	8	17	13	3400	1.26			
			10	9	23	17	3600	1.27			
			36	17	65	46	6200	1.30	0.33	6300	6800
4	150	0.6	4	5	4	5	2500	1.21			
			8	6	10	8	2900	1.25			
			10	6	13	9	3100	1.25			
			12	7	15	10	3300	1.27			
			36	12	27	18	5300	1.29	0.41	2800	3400

Conditions: [AIBN]/[xanthate] = 0.2, bulk, 65 °C. [a] Determined by $_1$H NMR in $CDCl_3$. [b] Determined by SEC in DMF/LiBr using a PS calibration. [c] Determined by $_1$H NMR in $CDCl_3$ (when f°_{DMOx} = 0-2) or DMSO-d6 (when f°_{DMOx} > 0.4), Mn NMR is measured considering the CH3O- chain-end signal h (Fig. S8af). d Theoretical molar mass calculated based on the [monomer]/[xanthate] ratio and the conversion.

Published in : Polymer Chemistry (2020), vol. 11, pp. 7207-7220
DOI: 10.1039/d0py01255f
Status : Postprint (Author's version)

Fig. 6 *(A) Dependence of M_n (full symbols) and Đ (hollow symbols) on the total monomer conversion for the RAFT of DMOx/VAc using $[monomers]_0/[xanthate]_0$ = 500 (■) or 150 (▲) (at 65 °C, f°_{DMOx} = 0:2, 0.2 eq. of AIBN (Table 4, entries 1 and 2). (B) SEC chromatograms for the RAFT of DMOx/VAc ($[monomers]_0/[xanthate]_0$ = 500, Table 4, entry 1).*

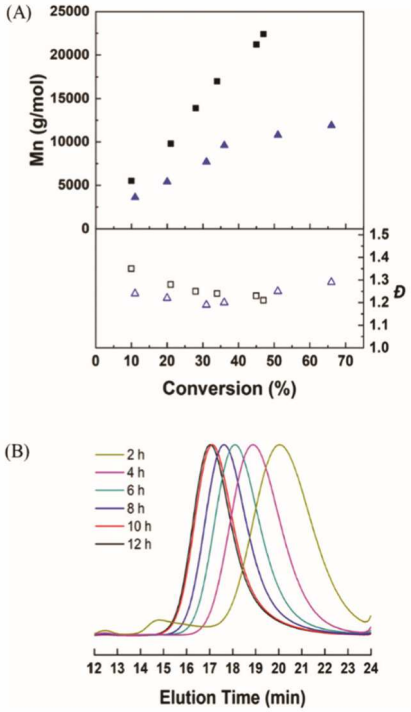

Published in : Polymer Chemistry (2020), vol. 11, pp. 7207-7220
DOI: 10.1039/d0py01255f
Status : Postprint (Author's version)

Fig. 7 *(A) Base hydrolysis of P(DMOx-co-VAc) prepared by RAFT (10 000 g mol^{-1}, f°_{DMOx} = 0.24) at different temperatures and (B) IR spectra of the copolymer precursor (black) and the resulting P(DMOxco-VA) (red) and P(AMBO-co-VA) (blue) copolymers.*

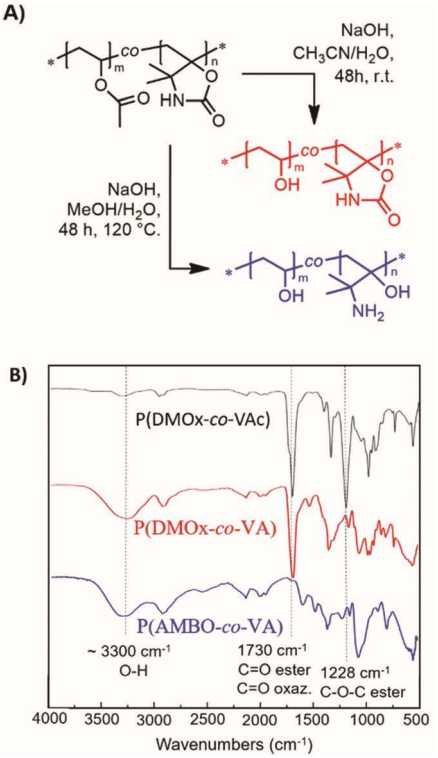

Published in : Polymer Chemistry (2020), vol. 11, pp. 7207-7220
DOI: 10.1039/d0py01255f
Status : Postprint (Author's version)

Fig. 8 *^{1}H NMR spectra of (A) P(DMOx-co-VAc) (M_n = 10 000 g mol^{-1}, f°_{DMOx} = 0.24) in DMSO-d_6, (B) P(DMOx-co-VA) in DMSO-d_6 and (C) P(AMBO-co-VA) in D_2O.*

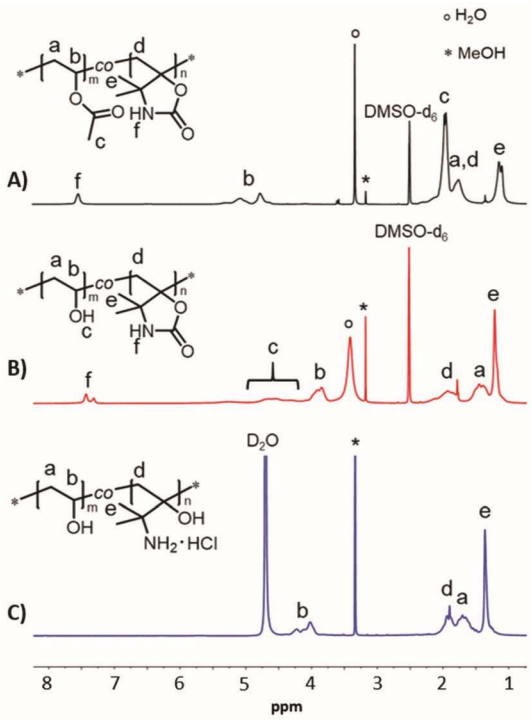

Published in : Polymer Chemistry (2020), vol. 11, pp. 7207-7220
DOI: 10.1039/d0py01255f
Status : Postprint (Author's version)

Fig. 9 *Illustration of the pH-, thermal- and metal-ion responsive behavior of the poly(AMBO-co-VA) in water. pH- and thermal-responsiveness of the copolymer solution (5 mg mL^{-1}) were followed by DLS. Metal-ion sensitivity of the poly(AMBO-co-VA) in water (2.5 mg mL^{-1}) was evidenced by addition of $CuCl_2$ (2 mg).*

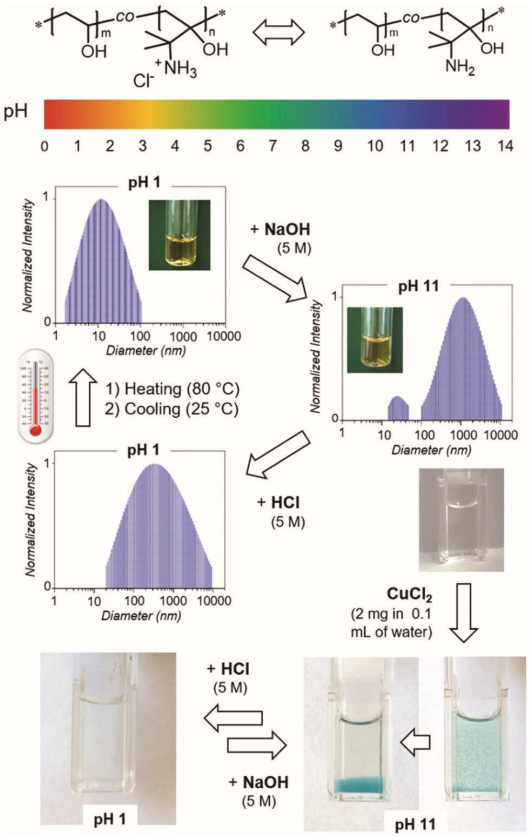

Conclusions

In summary, a methylene oxazolidinone compound, *i.e.* 4,4dimethyl-5-methyleneoxazolidin-2-one (DMOx), was considered as the (co)monomer in a radical polymerization process for the first time. DMOx was produced in high yield via an optimized procedure involving the silver-catalyzed carboxylative cyclization of dimethylpropargylamine. While polyDMOx could not be prepared by the conventional radical homopolymerization of DMOx, its copolymerization with VAc produced the targeted poly(DMOx-*co*-VAc) copolymers. In order to improve the control of the molecular parameters and composition of these copolymers, we considered some reversible deactivation radical polymerization methods and demonstrated the controlled radical copolymerization of DMOx and VAc by OMRP and RAFT using an alkyl-co(acac)$_2$ initiator and a xanthate chain transfer agent, respectively. The synthesis of well-defined poly(DMOx-co-VAc) copolymers was achieved by both

Published in : Polymer Chemistry (2020), vol. 11, pp. 7207-7220
DOI: 10.1039/d0py01255f
Status : Postprint (Author's version)

methods but RAFT appeared more suited than OMRP especially for high DMOx content. In the latter case, the OMRP polymerization notably slowed down during the polymerization suggesting that the optimum temperature range for the OMRP of non-conjugated monomers, i.e. 40–50 °C, is not favorable to the propagation of the DMOx. In contrast, the xanthate-mediated polymerization of LAMs, like VAc, typically operated at higher temperatures, above 60 °C. As a result, the RAFT of DMOx/VAc offered higher incorporation of DMOx into the copolymer while preserving a good level of control and decent rates of polymerization. These assumptions were supported by the DMOx/VAc reactivity ratios measured for both OMRP at 40 °C and RAFT at 65 °C. Next, chemical modifications of the poly(DMOx-co-VAc) copolymers gave access to unique modified poly(vinyl alcohol) derivatives. PVAs with pendant oxazolidinones as well as unprecedented vicinal amino alcohol-bearing PVAs, i.e. poly(AMBO-co-VA), were produced *via* base hydrolysis at 25 °C and 120 °C, respectively. Finally, we illustrated the multi-responsiveness of the fully hydrolyzed P(AMBO-co-VA) in water, i.e. pH-, thermal- and ionsensitivity. As anticipated, the increase of the pH triggered the deprotonation of the pendant ammonium moieties and the transition from free chains to micrometric objects. Interestingly, re-acidification of these solutions was not sufficient to disassemble all the objects; heating of the aqueous solutions was necessary to break the intermolecular H-bonding between the vicinal amino alcohol-containing copolymer chains. The metal-ion responsiveness of P(AMBO-*co*-VA) was also emphasized. In the presence of $CuCl_2$, a reversible transition was observed from free chains to crosslinked aggregates P(AMBO-*co*-VA) at pH 1 and 11, respectively, as a result of the specific chelation of Cu^{2+} ions by deprotonated amino groups. This characteristic could be developed and exploited in the future in the field of sensors and metal recovery systems. Overall, this work emphasizes the great potential of methylene oxazolidinones as building blocks in macromolecular engineering notably for the precision design of stimuli-responsive amino alcohol containing materials.

Conflicts of interest

There are no conflicts to declare.

Acknowledgements

The authors thank the Fonds de la Recherche Scientifique (FNRS) and the Fonds Wetenschappelijk Onderzoek – Vlaanderen (FWO) for funding the EOS project no O019618F (ID EOS: 30902231). A. D. and C. D. are Senior Research Associate and Research Director by F.R.S.-FNRS, respectively.

Published in : Polymer Chemistry (2020), vol. 11, pp. 7207-7220
DOI: 10.1039/d0py01255f
Status : Postprint (Author's version)

Notes and references

1. T. E. Smith , D. P. Richardson , G. A. Truran , K. Belecki and M. Onishi , J. Chem. Educ., 2008, 85 , 695
2. E. H. Tallmadge and D. B. Collum , J. Am. Chem. Soc., 2015, 137 , 13087
3. G. H. Wee and D. D. McLeod , J. Org. Chem., 2003, 68 , 6268
4. Z. Zhang and D. B. Collum , J. Am. Chem. Soc., 2019, 141 , 388
5. H. Adams , R. C. Collins , S. Jones and C. J. A. Warner , Org. Lett., 2011, 13 , 6576
6. K. Benakli , C. Zha and R. J. Kerns , J. Am. Chem. Soc., 2001, 123 , 9461
7. D. Crich and A. U. Vinod , Org. Lett., 2003, 5 , 1297
8. Bredikhin , Z. A. Bredikhina and A. T. Gubaidullin , Cryst. Eng. Comm., 2020, 10.1039/d0ce00116c
9. S. Baruah , M. Aier and A. Puzari , J. Heterocycl. Chem., 2020, 57 , 2498
10. D. Zhang , Y. Zhang , Y. Fan , M.-N. Rager , V. Guerineau , L. Bouteiller , M.-H. Li and C. M. Thomas , Macromolecules, 2019, 52 , 2719
11. D. E. Bergbreiter , A. M. Kippenberger and W. M. Lackowski , Macromolecules, 2005, 38 , 47
12. B. V. Lebedev , T. G. Kulagina , N. N. Smirnova , V. V. Veridusova , J. Kusan , H. Keul and H. Höcker , Macromol. Chem. Phys., 2000, 201 , 2469
13. K. Kim , D. Hwang , S. Kim , S. O. Park , H. Cha , Y.-S. Lee , J. Cho , S. K. Kwak and N.-S. Choi , Adv. Energy Mater., 2020, 10 , 2000012
14. H. Yeganeh , S. Jamshidi and P. H. Talemi , Eur. Polym. J., 2006, 42 , 1743
15. T. Pelzer , B. Eling , H.-J. Thomas and G. A. Luinstra , Eur. Polym. J., 2018, 107 , 1
16. Z. Liang , Z. Yang , S. Sun , B. Wu and L. R. Dalton , Chem. Mater., 1996, 8 , 2681
17. V. A. Sendijarevic , H. H. Lekovic and K. C. Frisch , J. Elastom. Plast., 1996, 28 , 63
18. V. A. Pankratov , T. M. Frenkel' and A. M. Fainleib , Russ. Chem. Rev., 1983, 52 , 576
19. Prokofyeva , H. Prokofyeva , D. J. Dijkstra , E. Frick , C. Guertler , C. Koopmans and A. Wolf , Polym. Int., 2017, 66 , 399
20. H. J. Altmann , M. Clauss , S. König , E. Frick-Delaittre , C. Koopmans , A. Wolf , C. Guertler , S. Naumann and M. R. Buchmeiser , Macromolecules, 2019, 52 , 487
21. J. E. Herweh and W. Y. Whitmore , J. Polym. Sci., Part A-1: Polym. Chem., 1970, 8 , 2759
22. D. J. Merline , C. P. Reghunadhan Nair , C. Gouri , R. Sadhana and K. N. Ninan , Eur. Polym. J., 2007, 43 , 3629
23. Y. Iwakura , S.-I. Izawa and F. Hayano , J. Polym. Sci., Part A-1: Polym. Chem., 1966, 4 , 751

Published in : Polymer Chemistry (2020), vol. 11, pp. 7207-7220
DOI: 10.1039/d0py01255f
Status : Postprint (Author's version)

24. Y. Iwakura and S.-I. Izawa , J. Org. Chem., 1964, 29 , 379
25. S. Gennen , B. Grignard , T. Tassaing , C. Jérôme and C. Detrembleur , Angew. Chem., Int. Ed., 2017, 56 , 10394
26. T. Endo , R. Numazawa and M. Okawara , Bull. Chem. Soc. Jpn., 1969, 42 , 1101
27. B. B. Wolfson and G. S. Banker , J. Pharm. Sci., 1965, 54 , 195
28. E. D. Little and D. Pickens , U.S. Patent , 3157668, 1961 .
29. Kutner J. Org. Chem., 1961, 26 , 3495
30. W. E. Walles and W. F. Tousignant , U.S. Patent , 2872321, 1958 .
31. J. F. Bork and L. E. Coleman , J. Polym. Sci., 1960, XLIII , 413
32. D. L. Trumbo Polym. Bull., 1993, 31 , 569
33. Atobe , T. Takata and T. Endo , J. Polym. Sci., Part A: Polym. Chem., 1993, 31 , 1543
34. S. Yamada , S. Nagai , K. Soraku and T. Endo , Polym. Bull., 2017, 74 , 2671
35. C. L. Mero and N. A. Porter , J. Org. Chem., 2000, 65 , 775
36. G. M. Miyake , D. A. DiRocco , Q. Liu , K. M. Oberg , E. Bayram , R. G. Finke , T. Rovis and E. Y-X. Chen , Macromolecules, 2010, 43 , 7504
37. T. Ishikawa , H. Nishizuka and T. Kawai , Bull. Chem. Soc. Jpn., 1988, 61 , 3559
38. T. Fujita and S. Yamago , Chem. – Eur. J., 2015, 21 , 18547
39. M. K. Akkapeddi Macromolecules, 1979, 505 , 546
40. Z. Vobecka , C. Wei , K. Tauer and D. Esposito , Polymer, 2015, 74 , 262
41. C. U. Pittman and H. Lee , J. Polym. Sci., Part A: Polym. Chem., 2003, 41 , 1759
42. M. K. Akkapeddi Polymer, 1979, 20 , 1215
43. Yoon , D. Jung , S. Lee , S. Lee , S. Choi , S. Woo and J. Moon , Proc. SPIE-Int. Soc. Opt. Eng., 2001, 4345 , 688
44. Kollar , M. Mrlik , D. Moravcikova , Z. Kronekova , T. Liptaj , I. Lac and J. Mosnacek , Macromolecules, 2016, 49 , 4047
45. B. Ramram , D. Chen , Y. Ma , L. Wang and W. Yang , J. Macromol. Sci., Part A: Pure Appl.Chem., 2016, 53 , 484
46. Moreno , M. Goikoetxea , J. C. de la Cal and M. J. Barandiara , Polym. Chem., 2014, 52 , 3543
47. R. A. Cockburn , R. Siegmann , K. A. Payne , S. Beuermann , T. F. L. Mckenna and R. A. Hutchinson , Biomacromolecules, 2011, 12 , 2319
48. G. M. Miyake , Y. Zhang and E. Y. Chen , J. Polym. Sci., Part A: Polym. Chem., 2015, 53 , 1523

Published in : Polymer Chemistry (2020), vol. 11, pp. 7207-7220
DOI: 10.1039/d0py01255f
Status : Postprint (Author's version)

49. G. M. Iskander , T. R. Ovenell and T. P. Davis , Macromol. Chem. Phys., 1996, 197 , 3123
50. Ueda , M. Honda , J.-I. Suciyama and H. Itoz , J. Polym. Sci., Part A: Polym. Chem., 1993, 31 , 949
51. M. Ueda and H. Mori , J. Polym. Sci., Part A: Polym. Chem., 1990, 28 , 2597
52. M. Heyns , R. Pfukwa and B. Klumperman , Biomacromolecules, 2016, 17 , 1795
53. B. V. Scholten , J. Demarteau , S. Gennen , J. D. Winter , B. Grignard , A. Debuigne , M. A. R. Meier and C. Detrembleur , Macromolecules, 2018, 51 , 3379
54. Cho and T. Lee , Makromol. Chem., Rapid Commun., 1989, 10 , 453
55. Mosnacek and K. Matyjaszewski , Macromolecules, 2008, 41 , 5509
56. Mosnacek , J. A. Yoon , J. Azhar , K. Kaloian and K. Matyjaszewski , Polymer, 2009, 50 , 2087
57. Juhari and J. Mosná , Polymer, 2010, 51 , 4806
58. Ding , A. John , J. Shin , Y. Lee , T. Quinn , W. B. Tolman and M. A. Hillmyer , Biomacromolecules, 2015, 16 , 2537
59. Y. Higaki , R. Okazaki and A. Takahara , ACS Macro Lett., 2012, 1 , 1124 CrossRef CAS .
60. T. Trotta , M. Jin , K. J. Stawiasz , Q. Michaudel , W. Chen and B. P. Fors , J. Polym. Sci., Part A: Polym. Chem., 2017, 55 , 2730
61. G. Qi , M. Nolan , F. J. Schork and C. W. Jones , J. Polym. Sci., Part A: Polym. Chem., 2008, 46 , 5929
62. S. Xu , J. Huang , S. Xu and Y. Luo , Polymer, 2013, 54 , 1779
63. Z. Wang , R. Poli , C. Detrembleur and A. Debuigne , Macromolecules, 2019, 52 , 8976
64. Demarteau , A. Debuigne and C. Detrembleur , Chem. Rev., 2019, 119 , 6906
65. Debuigne , C. Jérôme and C. Detrembleur , Polymer, 2017, 115 , 285
66. S. Perrier Macromolecules, 2017, 50 , 7433
67. R. Hill , R. N. Carmean and B. S. Sumerlin , Macromolecules, 2015, 48 , 5459
68. S. Harrisson , X. Lin , J.-N. Ollagnier , O. Coutelier , J.-D. Marty and M. Destarac , Polymer, 2014, 6 , 1437
69. Debuigne , Y. Champouret , R. Jérôme , R. Poli and C. Detrembleur , Chem. – Eur. J., 2008, 14 , 4046
70. Fineman and S. D. Ross , J. Polym. Sci., 1950, 5 , 259
71. T. Kelen and F. Tudos , J. Macromol. Sci. A, 1975, 9 , 1
72. Wamsley , B. Jasti , P. Phiasivongsa and X. Li , J. Polym. Sci., Part A: Polym. Chem., 2004, 42 , 317
73. J. M. Ting , T. S. Navale , F. S. Bates and T. M. Reineke , ACS Macro Lett., 2013, 2 , 770
74. J.-F. Qin , B. Wang and G.-Q. Lin , Green Chem., 2019, 21 , 4656 RSC .

Published in : Polymer Chemistry (2020), vol. 11, pp. 7207-7220
DOI: 10.1039/d0py01255f
Status : Postprint (Author's version)

75. H. Li , H. Feng , F. Wang and L. Huang , J. Org. Chem., 2019, 84 , 10380
76. T. Sakakura , J.-C. Choi and H. Yasuda , Chem. Rev., 2007, 107 , 2365
77. Yoshida , T. Mizuguchi and K. Shishido , Chem. – Eur. J., 2012, 18 , 15578
78. Y. Zhao , J. Qiu , Li. Tian , Z. Li , M. Fan and J. Wang , ACS Sustainable Chem. Eng., 2016, 4 , 5553
79. García-Domínguez , L. Fehr , G. Rusconi and C. Nevado , Chem. Sci., 2016, 7 , 3914 RSC .
80. K. Fujita , K. Inoue , J. Sato , T. Tsuchimoto and H. Yasuda , Tetrahedron, 2016, 72 , 1205
81. S. Ziane , M. M. Mazari , A. M. Safer , A. Sad El Hachemi Amar , S. Ruchaud , B. Baratte and S. Bach , Russ. J. Org. Chem., 2019, 55 , 1061
82. Brunel , J. Monot , C. E. Kefalidis , L. Maron , B. Martin-Vaca and D. Bourissou , ACS Catal., 2017, 7 , 2652
83. E. Jung and G. Piizzi , Chem. Rev., 2005, 105 , 1735
84. S. Yoshida , K. Fukui , S. Kikuchi and T. Yamada , Chem. Lett., 2009, 38 , 786
85. K. Sekine , R. Kobayashi and T. Yamada , Chem. Lett., 2015, 44 , 1407
86. T. Ishida , S. Kikuchi , T. Tsubo and T. Yamada , Org. Lett., 2013, 15 , 848
87. T. Ishida , R. Kobayashi and T. Yamada , Org. Lett., 2014, 16 , 2430
88. Debuigne , C. Jérôme and C. Detrembleur , Polymer, 2017, 115 , 285
89. J. Demarteau , P. B. V. Scholten , A. Kermagoret , J. D. Winter , M. A. Meier , V. Monteil , A. Debuigne and C. Detrembleur , Macromolecules, 2019, 52 , 9053
90. F.-S. Wang , T.-Y. Yang , C.-C. Hsu , Y.-J. Chen , M.-H. Li , Y.-J. Hsu , M.-C. Chuang and C.-H. Peng , Macromol. Chem. Phys., 2016, 217 , 422
91. G. Moad , E. Rizzardo and S. H. Thang , Polymer, 2008, 49 , 1079
92. S. Perrier Macromolecules, 2017, 50 , 7433
93. S. Harrisson , X. Liu , J.-N. Ollagnier , O. Coutelier , J.-D. Marty and M. Destarac , Polymer, 2014, 6 , 1437
94. H. Stenzel , L. Cummins , G. E. Roberts , T. P. Davis , P. Vana and C. Barner-Kowollik , Macromol. Chem. Phys., 2003, 204 , 1160
95. J. Chiefari , R. T. A. Mayadunne , C. L. Moad , G. Moad , E. Rizzardo , A. Postma , M. A. Skidmore and S. H. Thang , Macromolecules, 2003, 36 , 2273
96. S.-J. Katz and S.-C. Bergmeier , Tetrahedron Lett., 2002, 43 , 557
97. Debuigne , J.-R. Caille , N. Willet and R. Jérôme , Macromolecules, 2005, 38 , 9488
98. Detrembleur , O. Stoilova , R. Bryaskova , A. Debuigne , A. Mouithys-Mickalad and R. Jérôme , Macromol. Rapid Commun., 2006, 27 , 498

Published in : Polymer Chemistry (2020), vol. 11, pp. 7207-7220
DOI: 10.1039/d0py01255f
Status : Postprint (Author's version)

99. Bryaskova , N. Willet , A. Debuigne , R. Jérôme and C. Detrembleur , J. Polym. Sci., Part A: Polym. Chem., 2007, 45 , 81

100. M. I. Baker , S. P. Walsh , Z. Schwartz and B. D. Boyan , J. Biomed. Mater. Res., Part B, 2012, 100 , 1451

101. L. Bidault , M. Deneufchatel , C. Vancaeyzeele , O. Fichet and V. Larreta-Garde , Biomacromolecules, 2013, 14 , 3870

102. Kobayashi , K. D. Suh and Y. Shirokura , Macromolecules, 1989, 22 , 2363

103. X. Wang , S. Jing , Z. Hou , Y. Liu , X. Qiu , Y. Liu and Y. Tan , J. Mater. Sci., 2018, 53 , 15009 .